

## STEALTH GALAXIES IN THE HALO OF THE MILKY WAY

JAMES S. BULLOCK<sup>1</sup>, KYLE R. STEWART<sup>1</sup>, MANOJ KAPLINGHAT<sup>1</sup>, AND ERIK J. TOLLERUD<sup>1</sup>*Draft version January 9, 2019*

## ABSTRACT

We predict that there is a population of low-luminosity dwarf galaxies orbiting within the halo of the Milky Way that have surface brightnesses low enough to have escaped detection in star-count surveys. The overall count of stealth galaxies is sensitive to the presence (or lack) of a low-mass threshold in galaxy formation. These systems have luminosities and stellar velocity dispersions that are similar to those of known ultrafaint dwarf galaxies but they have more extended stellar distributions (half light radii greater than about 100 pc) because they inhabit dark subhalos that are slightly less massive than their higher surface brightness counterparts. As a result, the typical peak surface brightness is fainter than 30 mag per square arcsec. One implication is that the inferred common mass scale for Milky Way dwarfs may be an artifact of selection bias. If there is no sharp threshold in galaxy formation at low halo mass, then ultrafaint galaxies like Segue 1 represent the high-mass, early forming tail of a much larger population of objects that could number in the hundreds and have typical peak circular velocities of about  $8 \text{ km s}^{-1}$  and masses within 300 pc of about 5 million solar masses. Alternatively, if we impose a low-mass threshold in galaxy formation in order to explain the unexpectedly high densities of the ultrafaint dwarfs, then we expect only a handful of stealth galaxies in the halo of the Milky Way. A complete census of these objects will require deeper sky surveys, 30m-class follow-up telescopes, and more refined methods to identify extended, self-bound groupings of stars in the halo.

*Subject headings:* cosmology: theory — dark matter — galaxies: formation — galaxies: halos — methods: N-body simulations

## 1. INTRODUCTION

Approximately twenty-five new dwarf galaxy companions of the Milky Way (MW) and M31 have been discovered since 2004, more than doubling the known satellite population in the Local Group in five years (Willman et al. 2005; Zucker et al. 2006; Grillmair 2006; Majewski et al. 2007; Belokurov et al. 2007; Grillmair 2009; Belokurov et al. 2009; Martin et al. 2009). The majority of these newly-discovered dwarfs are less luminous than any galaxy previously known. The most extreme of these, the ultrafaint MW dwarfs, have luminosities smaller than an average globular cluster  $L_V \simeq 10^2 - 10^4 L_\odot$ , and were discovered by searches for stellar overdensities in the wide-field maps of the Sloan Digital Sky Survey (SDSS) and the Sloan Extension for Galactic Understanding and Exploration (SEGUE). Follow-up kinematic observations showed that these tiny galaxies have surprisingly high stellar velocity dispersions for their luminosities and sizes ( $\sigma_\star \sim 5 \text{ km s}^{-1}$ , Martin et al. 2007; Simon & Geha 2007; Geha et al. 2009) and subsequent mass modeling has shown that they are the most dark matter dominated galaxies known (Strigari et al. 2008; Wolf et al. 2009). Remarkably, these extreme systems are not only the faintest, most dark matter dominated galaxies in the universe but they are also the most metal poor stellar systems yet studied (Kirby et al. 2008; Geha et al. 2009).

Perhaps the most exciting aspect of these recent discoveries is that they point to a much larger population. Detection in the SDSS is complete only to  $\sim 50 \text{ kpc}$  for the least luminous dwarfs (Koposov et al. 2008; Walsh et al. 2009) and straightforward cosmologically motivated luminosity bias and coverage corrections

suggest that there are  $\sim 500$  ultrafaint dwarf galaxies within 400 kpc of the Milky Way (Tollerud et al. 2008), with an ever increasing number beyond. Moreover, the luminosity-distance detection limits only apply for systems with peak surface brightness obeying  $\mu_V < 30 \text{ mag arcsec}^{-2}$  (Koposov et al. 2008). Any satellite galaxy with a luminosity of  $L \sim 1000 L_\odot$  and a projected half-light radius  $R_e$  larger than about 100 pc would have evaded detection with current star-count techniques regardless of its distance from the Sun.

Here we argue that there should be a population of dwarf galaxies surrounding the Milky Way (and by extension, throughout the universe) that are so diffuse in stellar density that they would have thus far avoided discovery. Our predictions rely on the fact that the effective radius  $R_e$  of a dark matter dominated, dispersion-supported galaxy with fixed stellar velocity dispersion will increase as its dark matter halo mass decreases. One implication of this idea is that the known ultrafaint dwarf spheroidals (dSphs) may represent the high (dark matter) mass tail of a larger distribution of stealth galaxies. These undiscovered systems should preferentially inhabit the lowest mass dark matter subhalos that host stars, and may provide an important missing link for the satellite-subhalo problem in Cold Dark Matter (CDM) models (Klypin et al. 1999; Moore et al. 1999; Bullock et al. 2000; Stoehr et al. 2002; Zentner & Bullock 2003; Kazantzidis et al. 2004; Strigari et al. 2007; Macciò et al. 2009; Busha et al. 2009; Muñoz et al. 2009; Kravtsov 2009; Okamoto & Frenk 2009).

Mass determinations for MW dSphs based on current stellar kinematic samples reveal a surprising lack of trend between inferred dark matter halo masses and galaxy luminosities (Strigari et al. 2008; Peñarrubia et al. 2008; Walker et al. 2009; Wolf et al. 2009). The tiniest satel-

<sup>1</sup> Center for Cosmology, Department of Physics and Astronomy, The University of California at Irvine, Irvine, CA, 92697, USA; bullockuci.edu

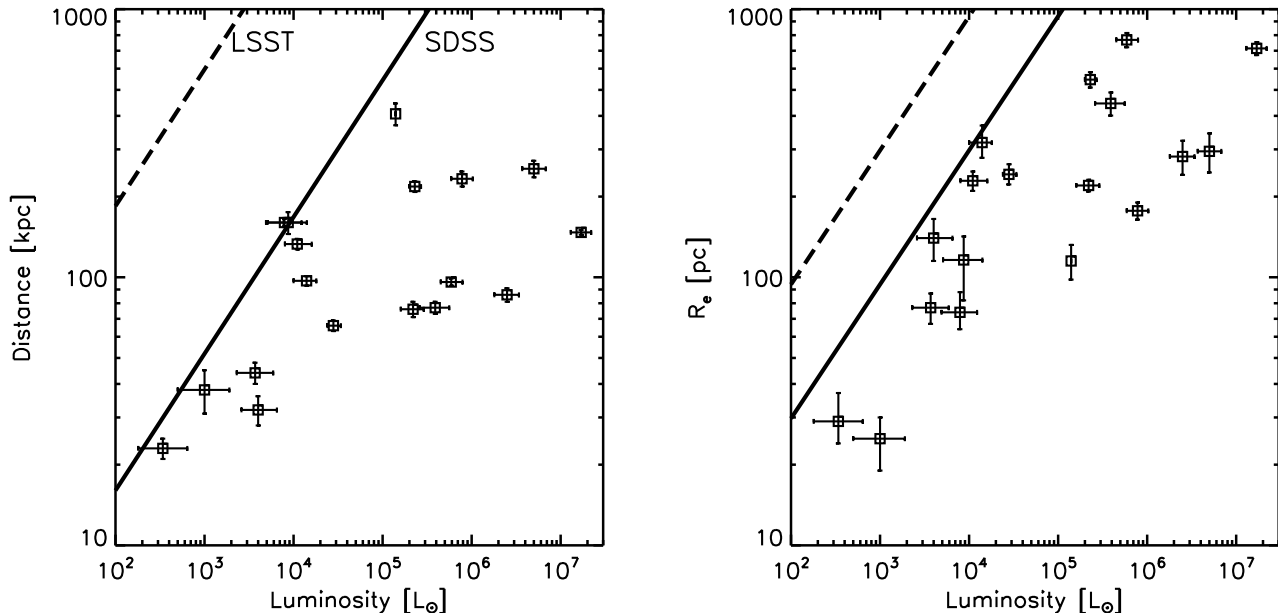


FIG. 1.— Projected helio-centric distance vs. V=band luminosity (left) and half-light radius  $R_e$  vs. V-band luminosity (right) for Milky Way dSph galaxies. The lines in the left panel show SDSS luminosity completeness limits from Walsh et al. (2009) and an estimate for LSST completeness following Tollerud et al. (2008). In the right panel, galaxies above the solid line, with surface brightness fainter than  $\mu = 30$  mag arcsec $^{-2}$  are currently undetectable. For reference, the dashed line in the right panel corresponds to  $\mu = 35$  mag arcsec $^{-2}$ .

lite galaxies have dark matter densities indicative of dark matter halos that are at least as massive as those of systems 10,000 times more luminous. For example, Strigari et al. (2008) found that the integrated mass within 300 pc for each galaxy shows no evidence for a relationship with luminosity:  $M_{300} \propto L^{0.03 \pm 0.03}$ . The radius 300 pc provides a good benchmark radius for comparison for two reasons. First, it represents a typical three-dimensional half-light radius for the bulk population of MW dSphs (Strigari et al. 2008; Wolf et al. 2009), and second, it is the largest radius that can currently be well-resolved in CDM N-body simulations (Springel et al. 2008 and Diemand et al. 2008). There are four galaxies that lack stellar tracers that extend to 300 pc. In these cases, the inferred mass within 300 pc requires an extrapolation based on a physically-motivated prior (Strigari et al. 2008). Such an extrapolation is perfectly reasonable because CDM subhalos have strong (predicted) correlations between the density at some inner radius (e.g. 100 pc) and at a larger radius (e.g. 300 pc) and we aim to compare to CDM predictions. Moreover, even the closest galaxy, Segue I, has a minimum instantaneous tidal radius that is larger than 300 pc.

The normalization of the  $M_{300} - L$  relation at  $M_{300} \simeq 10^7 M_\odot$  is indicative of the central densities of *massive* dark matter subhalos ( $V_{\max} \gtrsim 15$  km s $^{-1}$ ) and is fairly easy to explain in  $\Lambda$ CDM models (Strigari et al. 2008; Macciò et al. 2009; Busha et al. 2009; Muñoz et al. 2009; Kravtsov 2009; Li et al. 2009; Okamoto & Frenk 2009; Stringer et al. 2009). However, the lack of observed correlation between  $L$  and mass is quite unexpected. To put the lack of measured slope in the  $M_{300} - L$  relation in perspective, consider the relationship between dark matter halo  $V_{\max}$  and galaxy luminosity required to match the faint-end slope of the galaxy luminosity function:

$L \propto V_{\max}^b$  with  $b = 7.1$  (Busha et al. 2009). Tully-Fisher studies suggest an even flatter relation, with  $b \simeq 4$  (e.g., Stark et al. 2009; Courteau et al. 2007). For dark matter halos of interest, with maximum circular velocities  $V_{\max} \simeq 15 - 45$  km s $^{-1}$ , we expect  $M_{300} \propto V_{\max}$  (assuming NFW fits to halos in Springel et al. 2008) such that the observed trend  $M_{300} \propto L^{0.03}$  would naively imply  $L \propto V_{\max}^b$  with  $b \simeq 33$ . This is a much steeper relationship than we expect from more luminous systems. We emphasize that the lack of inferred relationship between dSph luminosity and halo mass is not an artifact of the specific choice of 300 pc for the mass comparison. Indeed, if one performs the same comparison between galaxies using a smaller benchmark radius (100 pc, Strigari et al. 2008) or using the 3d half-light radius for each galaxy (Wolf et al. 2009) or using the 3d mass within the 2d half-light radius of each galaxy (Walker et al. 2009) then one reaches the same conclusion: there is no observed trend between inferred halo mass (or  $V_{\max}$ ) and luminosity.

One possible explanation for this lack of mass trend is that it reflects a scale in galaxy formation, where the scatter in  $L$  at fixed  $V_{\max}$  becomes very large, as might possibly be explained by feedback due to photoionization or suppression below the atomic cooling limit (Strigari et al. 2008; Macciò et al. 2009; Okamoto & Frenk 2009; Stringer et al. 2009, and §3 below). Another possibility, outlined below, is that the lack of an observed trend between mass and luminosity is the product of selection bias: most ultrafaint galaxies do inhabit halos with  $M_{300} \lesssim 10^7 M_\odot$ , but they are too diffuse to have been discovered.

In the next section, we explain why we expect surface brightness selection bias to limit the discovery of satellite galaxies in small subhalos. In §3 we use a sim-

ple model to estimate the number of low surface brightness stealth galaxies within the vicinity of the Milky Way. Our estimates rely on the public subhalo catalogs provided by the Via Lactea 2 N-body simulation group (Diemand et al. 2008). We explore two models. Our Fiducial Scenario connects each subhalo’s mass and accretion time to a galaxy luminosity  $L$  by extrapolating the halo mass-light relationship required to match the asymptotic slope of the galaxy stellar mass function (Moster et al. 2009). Our secondary model (Threshold Scenario) explores a scenario where galaxy formation is truncated sharply below a characteristic dark halo mass scale. We present our findings in §4 and conclude in §5.

## 2. MOTIVATIONS

The left panel of Figure 1 shows the known MW dSphs plotted in the plane of helio-centric distance vs. V-band luminosity. The solid line (labeled SDSS) illustrates the distance to which dwarfs of a given luminosity can be detected in SDSS with 90% efficiency from Walsh et al. (2009). Similar results were presented by Koposov et al. (2008). The upper line shows the same limit adjusted up by scaling to the limiting magnitude of the full co-added LSST survey (Tollerud et al. 2008; Ivezić et al. 2008). Clearly, the known dwarf galaxies cluster at the current completeness edge of the diagram, indicating a high likelihood for future discoveries (Koposov et al. 2008; Tollerud et al. 2008; Walsh et al. 2009).

The distance-luminosity completeness limits presented by Walsh et al. (2009) and Koposov et al. (2008) are only applicable for systems with surface brightness brighter than  $\mu_V = 30$  mag arcsec $^{-2}$  (Koposov et al. 2008, and G. Gilmore, M. Geha, and B. Willman, private communications). Systems more diffuse than this limit cannot be detected in SDSS with current methods, no matter their helio-centric distance. This phenomenon is illustrated qualitatively in the right panel of Figure 1, which presents the same set of MW dSphs in the plane of  $R_e$  vs.  $L$ . The solid line shows a constant peak (central) surface brightness for a Plummer profile

$$\Sigma_{\text{peak}} = \frac{L}{\pi R_e^2} = 0.036 L_{\odot} \text{ pc}^{-2}, \quad (1)$$

and corresponds to  $\mu_V = 30$  mag arcsec $^{-2}$  for solar absolute magnitude  $M_{\odot V} = 4.83$ . As in the distance-luminosity figure, the tendency for many of the fainter dwarfs to “pile up” near the surface brightness detection limit is suggestive. There is nothing ruling out the presence of a larger population of more extended systems that remain undetected because of their low surface brightness.

If a large number of diffuse, undetected galaxies do exist, they are likely associated with low-mass dark matter subhalos. One can understand this expectation by considering a spherically-symmetric galaxy with stellar density distribution  $\rho_*(r)$  and radial velocity profile  $\sigma_r(r)$  that is embedded within a gravitationally-dominant dark matter halo mass profile  $M(r)$ . The Jeans equation implies

$$M(r) = \frac{r \sigma_r^2}{G} (\gamma_* + \gamma_\sigma - 2\beta), \quad (2)$$

where  $\beta(r) \equiv 1 - \sigma_t^2/\sigma_r^2$  characterizes the tangential velocity dispersion and  $\gamma_* \equiv -d \ln \rho_*/d \ln r$  and  $\gamma_\sigma \equiv$

$-d \ln \sigma_r^2/d \ln r$ . If we make the simplifying assumption that  $\beta = 0$  and  $\sigma(r) \simeq \sigma_* = \text{constant}$ , with  $\gamma_\sigma \ll 1$  then  $M(r) = r G^{-1} \sigma_*^2 \gamma_*$ . For a fixed velocity dispersion, a more spatially extended profile (smaller  $\gamma_*$ ) requires a lower mass at fixed radius.

The same basic expectation follows in a more general context from the recent work of Wolf et al. (2009), who showed<sup>2</sup> that the total mass of a quasi-spherical dSph galaxy within its 3d half-light radius  $r_{1/2} \simeq 1.3 R_e$  may be determined accurately from the luminosity weighted line-of-sight velocity dispersion  $\sigma_*$  for general  $\beta$ :  $M(r_{1/2}) = 3 G^{-1} r_{1/2} \sigma_*^2$ . Mass determinations at larger and smaller radii require an extrapolation of the mass profile from that point, but given a theoretical prediction for the mass profile shape  $M(r)$  one can perform this extrapolation by simply normalizing at  $r = r_{1/2}$ .

It is useful to rewrite the Wolf et al. (2009) mass estimator in terms of the implied circular velocity at  $r_{1/2}$ :

$$V_c(r_{1/2}) = \sqrt{3} \sigma_*. \quad (3)$$

Consider then a galaxy with velocity dispersion  $\sigma_*$  and luminosity  $L$  embedded within a gravitationally-dominant dark matter halo described by a circular velocity curve that increases with radius as an approximate power law:  $V_c(r) = V_{300} (r/300 \text{ pc})^\alpha$ . Equation 3 implies  $r_{1/2} = 300 \text{ pc} (\sqrt{3} \sigma_*/V_{300})^{1/\alpha}$ . For an NFW halo (Navarro et al. 1997) with  $r_s \gg 300 \text{ pc}$  we have  $\alpha = 1/2$  and  $r_{1/2} \propto V_{300}^{-2} \propto M_{300}^{-1}$ . Clearly, the galaxy becomes puffier as we decrease  $M_{300}$  or  $V_{300}$ . One implication is that if a galaxy has a stellar density that is just large enough to be detected, another galaxy with identical  $L$  and  $\sigma_*$  will be undetectable if it happens to reside within a slightly less massive halo.

Figure 2 provides a more detailed exploration of the relationship between halo mass parameters ( $M_{300}$  or  $V_{\text{max}}$ ) and associated dSph observables  $\sigma_*$ ,  $L$ , and  $R_e$ . Points in the left panel of Figure 2 present  $M_{300}$  vs.  $L$  for MW dSph galaxies, with masses from Strigari et al. (2008) and luminosities updated as in Wolf et al. (2009). The right panel shows  $\sigma_*$  vs.  $L$  for the same galaxies culled from Table 1 of Wolf et al. (2009).

The shaded bands and dashed lines in each panel of Figure 2 illustrate the way in which surface brightness incompleteness may affect these diagrams. In determining these regions we have assumed each dSph is dark-matter dominated, such that its gravitating mass profile produces an NFW circular velocity curve  $V_c(r) = V_{\text{NFW}}(r)$ . Given the NFW shape, the rotation curve is fully specified by its peak value  $V_{\text{max}}$  and the radius where the peak occurs  $r_{\text{max}}$  (e.g., Bullock et al. 2001). We assume for simplicity that subhalos of a given  $V_{\text{max}}$  map in a one-to-one way to a rotation curve shape using  $r_{\text{max}} = 650 \text{ pc} (V_{\text{max}}/10 \text{ km s}^{-1})^{1.35}$ , which is indicative of median subhalos in high-resolution N-body simulations (intermediate between the normalizations of Springel et al. 2008 and Diemand et al. 2008). With this assumption in place, given a halo mass variable (e.g.,  $M_{300}$  or  $V_{\text{max}}$ ), we may determine the implied half-light radius  $R_e \simeq 0.75 r_{1/2}$  associated with any  $\sigma_*$  using

<sup>2</sup> Under the assumption that the observed stellar velocity dispersion remains fairly flat with projected radius, as is the case with all of the well-studied systems.

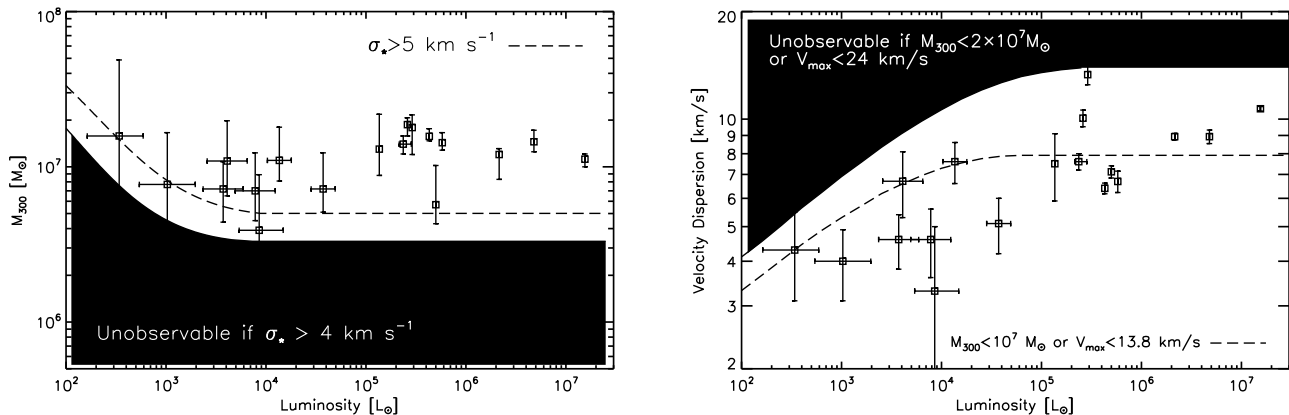


FIG. 2.— Mass within 300 pc vs. luminosity (left) and measured stellar velocity dispersion,  $\sigma_*$ , vs. luminosity (right) for Milky Way dwarf spheroidal galaxies (data points with error bars). In the left panel, galaxies within the shaded region (below dashed line) will remain hidden ( $\mu > 30$  mag arcsec $^{-2}$ ) if they have  $\sigma_* > 4$  km s $^{-1}$  ( $\sigma_* > 5$  km s $^{-1}$ ). In the right panel, galaxies in the shaded region will be stealth ( $\mu > 30$ ) if they have  $M_{300} < 2 \times 10^7 M_\odot$  and galaxies below the dashed line will be stealth if they have  $M_{300} < 10^7 M_\odot$ . The masses and velocity dispersions quoted here are taken from Strigari et al. (2008) and Wolf et al. (2009). Since the time of those publications, it has come to our attention that the velocity dispersion (and hence mass) errors on Hercules (at  $L \simeq 3 \times 10^4 L_\odot$ , Adén et al. 2009) and W1 (at  $L \simeq 10^3 L_\odot$ , B. Willman & M. Geha, private communications) are likely underestimated because of membership uncertainties.

$V_{\text{NFW}}(r_{1/2}) = \sqrt{3} \sigma_*$  (Equation 3).

In the right panel of Figure 2, galaxies residing in the shaded region are unobservable if they sit within dark matter halos less massive than  $M_{300} = 2 \times 10^7$  or (equivalently for our assumptions) with peak circular velocity smaller than  $V_{\text{max}} = 24$  km s $^{-1}$ . Similarly, galaxies residing above the dashed line are too diffuse to be detected if they have  $M_{300} < 10^7 M_\odot$  or  $V_{\text{max}} \lesssim 14$  km s $^{-1}$ . Galaxies need to have deep potential wells if they are to remain observable at low luminosity for  $\sigma_* \sim 5$  km s $^{-1}$ . If there are low-luminosity galaxies with  $M_{300}$  values smaller than  $\sim 10^7 M_\odot$  they would remain hidden as long as they have stellar velocity dispersions comparable to those of the known dwarfs.<sup>3</sup>

A related set of limits in the  $M_{300} - L$  plane is depicted in the left panel of Figure 2. Galaxies sitting in the shaded band will have  $R_e$  too large to be observable if they have  $\sigma_* > 4$  km s $^{-1}$ . Slightly hotter galaxies, with  $\sigma_* > 5$  km s $^{-1}$  will be unobservable if they sit below the dashed line. As expected, the hotter the galaxy, the deeper the potential well needs to be in order keep the stars confined to an observable surface brightness. We see that galaxies with  $L \sim 10^3 L_\odot$  residing in a halos less massive than  $M_{300} \simeq 8 \times 10^6 M_\odot$  will be too diffuse to be seen if they have  $\sigma_* = 5$  km s $^{-1}$ . Note that for  $L \gtrsim 10^4 L_\odot$  the constraint on allowed  $M_{300}$  values is flat with  $L$  because halos smaller than this value are kinematically forbidden via Equation 3. Specifically, kinematic mass determinations demand  $V_{\text{max}} \geq \sqrt{3} \sigma_*$ .

Implicit in the above discussion is the idea that a galaxy's  $\sigma_*$  can be considered independently of its halo mass. Dynamically, the only constraint is that  $\sigma_* \leq V_{\text{max}}/\sqrt{3}$  (Equation 3). One is more inclined to suspect that  $\sigma_*$  in an ultrafaint dSph is governed by star

formation and galaxy formation processes, with an absolute minimum set by the effective temperature of the star forming ISM. Even for a very cold primordial effective ISM temperature,  $T_{\text{ISM}} \sim 300$  K, we expect  $\sigma_{\text{ISM}} \sim 2$  km s $^{-1}$ , and this ignores turbulent and magnetic pressure terms. The vast majority of globular clusters have stellar velocity dispersions larger than this (Pryor & Meylan 1993). Moreover, dark matter halos of all masses are expected to have experienced significant mergers in their early histories (e.g., Stewart et al. 2008). These mergers would have heated (the oldest) stars beyond any primordial pressurized motions. This realization is important because larger  $\sigma_*$  values will produce more extended stellar distributions within dark halos of fixed mass. In the next section we consider the implications of a model where  $\sigma_*$  is correlated with luminosity  $L$  in a way that tracks the observed relationship (right panel of Figure 2). In principle, there could be a floor in the  $\sigma_*$  values allowed for dwarf galaxies. We do not impose such a floor in our calculations, but if one does exist, then our estimates could *under-predict* the fraction of stealth galaxies at low luminosities.

### 3. MODEL

We rely on the publicly released subhalo catalogs of the Via Lactea II N-body simulation (VL2 hereafter) as described in Diemand et al. (2008). The simulation adopts cosmological parameters from WMAP3 (Spergel et al. 2007) and tracks the formation of a Milky Way size dark matter halo with a highest particle-mass resolution of  $4,100 M_\odot$  and force resolution of 40 pc. The main halo has a radius of 402 kpc, defined to enclose a mean density that is 200 times the mean matter density of the universe, and an associated mass of  $M_{\text{halo}} = 1.9 \times 10^{12} M_\odot$ . The public subhalo catalogs include  $M_{300}$ ,  $V_{\text{max}}$ , and  $r_{\text{max}}$  parameters for each bound system, as well as merger history information that allows us to track the redshift of infall  $z_{\text{inf}}$  for each subhalo and to determine its maximum attained mass  $M_{\text{max}}$  prior to infall. Tests by the VL2 team suggest that the measured  $M_{300}$  masses are good to about 20% (random) owing to resolution effects

<sup>3</sup> In deriving these regions, we have explicitly assumed that the stellar systems are dark-matter dominated within their half-light radii. The same arguments cannot be applied to globular cluster systems, some of which do inhabit the shaded regions in the right panel of Figure 2 without any discernible dark matter halo. These systems have large velocity dispersions simply because they have very high stellar densities.



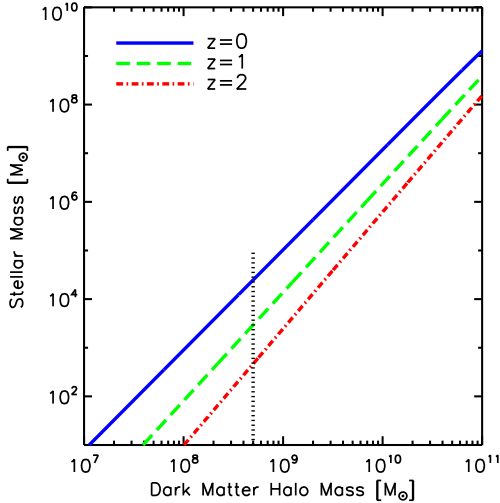


FIG. 3.— Model stellar mass - halo mass relation (Moster et al. 2009) shown at three example redshifts. Our Fiducial Scenario assumes that the  $M_{\text{halo}}-M_*$  relation extrapolates smoothly to very small masses. Our Threshold Scenario imposes a sharp truncation mass at  $M_{\text{halo}} = 5 \times 10^8 M_{\odot}$  (vertical dotted line) below which all halos are assumed to form no stars.

(J. Diemand, private communication).

We assign light to each of our accreted dark matter subhalos by assuming that at each redshift  $z$  there is a monotonic relationship between halo mass  $M_{\text{halo}}$  and galaxy stellar mass  $M_*$ . This general approach is motivated by its demonstrated success in producing the clustering properties of galaxies larger than  $M_* \simeq 10^9 M_{\odot}$  (Kravtsov et al. 2004; Tasitsiomi et al. 2004; Vale & Ostriker 2004; Conroy et al. 2006; Berrier et al. 2006; Purcell et al. 2007; Marín et al. 2008; Stewart et al. 2009; Conroy & Wechsler 2009). Of course, cosmological abundance matching cannot be applied directly at the smallest stellar masses because of completeness issues. In our Fiducial Scenario we simply adopt the asymptotic  $M_{\text{halo}} - M_*$  relationship suggested by the most complete stellar mass functions, which effectively assumes that there is no new (or abrupt) mass scale that truncates galaxy formation in small halos. We also explore a Threshold Scenario that imposes such a truncation scale (see below).

For our Fiducial Scenario, we assign  $M_*$  to each subhalo by extrapolating the fitting formula presented by Moster et al. (2009) to small stellar masses. Moster et al. (2009) derived the relationship using N-body halo catalogs together with observationally inferred stellar mass functions for  $M_* \gtrsim 10^{8-9} M_{\odot}$  galaxies out to redshift  $z \sim 3$ . The implied (extrapolated) relationship between stellar mass and dark halo mass is presented in Figure 3 for three example redshifts. We see that  $M_*$  must decrease at high redshift for a fixed  $M_{\text{halo}}$  in order to explain the evolving stellar mass function. Low-mass halos at high redshift have not had time to form as many stars as their  $z \sim 0$  counterparts. For our Threshold Scenario we adopt the same mapping for massive halos but we impose a sharp truncation in the  $M_* - M_{\text{halo}}$  relation at  $M_{\text{halo}} = 5 \times 10^8 M_{\odot}$  (dotted line in Figure 3).

We assume that star formation is quenched in each subhalo at a time  $\tau_q$  after the redshift of accretion into

the VL2 host. Specifically, subhalo light content is determined at redshift  $z_q$  (set at a time  $\tau_q$  after the accretion redshift) using the appropriate Moster et al. (2009) mapping with  $M = M_{\text{max}}$ , the maximum mass each subhalo progenitor obtained prior to infall. If the subhalo is accreted at a time less than  $\tau_q$  before  $z = 0$  we adopt the Moster et al. (2009) relation at  $z_q = 0$ . For the figures we present below we use a quenching timescale that is roughly a dynamical time for the host halo  $\tau_q = 2$  Gyr. We find that the value of  $\tau_q$  only affects our predictions for the largest satellites  $M_* \gtrsim 10^6 M_{\odot}$ . For example, if we set  $\tau_q = 0$ , we under-predict the number of luminous satellites by a few, but the low-luminosity satellite count is largely unaffected. The main conclusions of this paper regarding the least luminous, stealth satellites are not sensitive to the choice of  $\tau_q$ . For all satellites, we convert from stellar mass to V-band luminosity using  $M_*/L = 2 [M_{\odot}/L_{\odot}]$ , which is typical for Milky Way dSphs according to Martin et al. (2008) for a Kroupa IMF.

Once  $L$  is determined for each subhalo, we assign a stellar velocity dispersion by adopting the empirical relation shown in the right panel of Figure 2:

$$\sigma_* = 6.9 \text{ km s}^{-1} \left( \frac{L}{10^5 L_{\odot}} \right)^{0.09}, \quad (4)$$

with a log normal scatter of  $\Delta \log_{10} \sigma = 0.1$  at fixed  $L$ .<sup>4</sup> We then determine  $R_e \simeq 0.75 r_{1/2}$  using  $V_{\text{NFW}}(r_{1/2}) = \sqrt{3} \sigma_*$  (Equation 2). The  $V_{\text{max}}$  and  $r_{\text{max}}$  values that define  $V_{\text{NFW}}(r)$  are those measured for each subhalo in the simulation. For simplicity, we assume that each dwarf galaxy follows a Plummer profile, with a peak surface density given by Equation 1. As discussed above, galaxies with  $\Sigma_{\text{peak}} < 0.036 L_{\odot} \text{ pc}^{-2}$  are assumed to be undetectable with standard techniques. We note that if we impose a floor in allowed velocity dispersions near  $\sigma_* = 4 \text{ km s}^{-1}$  then our results do not change dramatically.

The final step in our procedure is to check that our implied  $r_{1/2}$  values are small enough for our galaxies to be relatively unaffected by tidal stripping. In order to do this we estimate a tidal radius for each galaxy  $r_t$  and remove galaxies from our catalogs if  $r_{1/2} > r_t$  on the assumption that most of their stars will have been tidally liberated (even though a dark matter core remains bound). It is well known a subhalo's rotation curve should decline more rapidly than an NFW profile for  $r \gtrsim r_{\text{max}}$  because of tidal effects (Kazantzidis et al. 2004). This means that  $r_t = r_{\text{max}}$  provides a reasonable estimate for the gravitational tidal radius of a galaxy embedded within that subhalo. We find that 2% (10%) of our galaxies with  $L > 100 L_{\odot}$  ( $10 L_{\odot}$ ) have  $r_{1/2} > r_{\text{max}}$ , and that the majority of these systems have lost more than 90% of their dark matter mass since falling into the host. Physically, these objects with  $r_{1/2} > r_{\text{max}}$  represent systems that are losing stellar material. We will not explore the observational implications of this evaporating

<sup>4</sup> We do not account for any systematic surface brightness bias that would lead to high  $\sigma_*$  systems being missed (as these are the systems that will have large  $R_e$ ). By ignoring this effect we are systematically *under-estimating* the possible number of stealth galaxies.

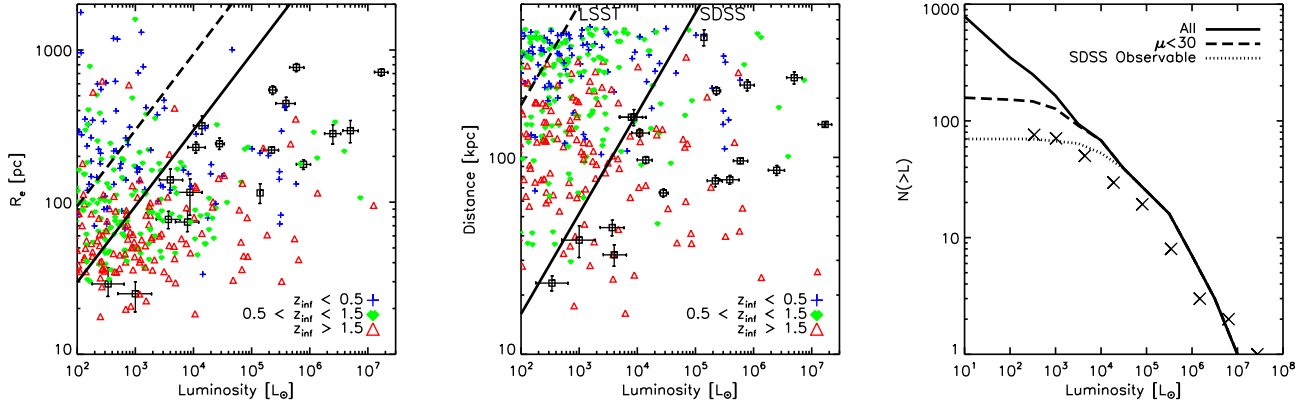


FIG. 4.— Fiducial Scenario galaxy size vs. luminosity relation (colored points, left); distance vs. luminosity relation (middle); and luminosity functions for different completeness cuts (right). *Left Panel:* The solid line corresponds to the current detection limit at a peak surface brightness of  $\mu = 30$  mag arcsec $^{-2}$  and the dashed line corresponds to  $\mu = 35$  mag arcsec $^{-2}$ , for reference. The small colored points represent model galaxies and the point-type scheme maps to the redshift of infall into the host dark halo: open triangles have  $z_{\text{inf}} > 1.5$ , green diamonds have  $0.5 \leq z_{\text{inf}} \leq 1.5$ , and blue pluses were accreted since  $z = 0.5$ . The black squares with error bars are known MW dSph galaxies. *Middle Panel:* The solid and dashed lines indicate luminosity-distance completeness in the SDSS and LSST, respectively, for systems with  $\mu < 30$  mag arcsec $^{-2}$ . The point types are the same as in the left panel. *Right Panel:* The symbols shown as X's reflect the current census of MW dSphs, corrected for the sky coverage completeness of SDSS as in Tollerud et al. (2008). The uncertainty in this correction corresponds roughly to the size of the symbols we use. The dotted line shows the predicted cumulative luminosity function of satellite galaxies that are bright enough to have been detected by SDSS according to the Walsh et al. (2009) limits. The dashed line shows the predicted luminosity function of all satellites with surface brightness meeting the  $\mu < 30$  mag arcsec $^{-2}$  threshold, most of which should be detectable by LSST. The solid line shows all satellite galaxies, including the stealth population. We see that the majority of ultrafaint dwarfs are expected to have surface brightnesses so low that they will avoid detection without revised techniques for discovery.

population here, but this definition may prove useful for future theoretical explorations aimed at predicting the fraction of dwarf satellites that should be showing signs of ongoing stellar stripping. By excluding these stripped galaxies from our estimates we are being conservative in our estimates of the stealth population.

Before moving on to our results, we mention that the halo finder and the associated definition of halo mass used by Moster et al. (2009) in our stellar mass assignment differ slightly from those used in the VL2 catalogs. We estimate that this amounts to a  $\sim 20\%$  difference in dark matter halo mass association for any individual object, a difference that is not significant given the exploratory nature of this work.

#### 4. RESULTS

Figure 4 provides a summary of our fiducial model predictions compared to current observations: galaxy  $R_e$  vs. luminosity (left), helio-centric distance vs. luminosity (middle), and cumulative number vs. luminosity (right). The small colored symbols in the left and middle panels are model galaxies, with color and symbol type indicating three infall redshift bins with  $z_{\text{inf}} > 1.5$  (red triangles),  $0.5 \leq z_{\text{inf}} \leq 1.5$  (green diamonds), and  $z < 0.5$  (blue pluses). The larger, black squares reproduce the MW dSph data from Figure 1. In the middle panel, the helio-centric distance for model galaxies is measured from an arbitrary point 8 kpc from the host dark matter halo center. Our gross results are independent of this choice for solar location.

Model galaxies above the solid line in the left panel of Figure 4 are too diffuse to have been detected. Clearly, this population is significant. At fixed luminosity, systems above the solid line ( $\mu = 30$  mag arcsec $^{-2}$ ) tend to have been accreted more recently (blue pluses) than their higher-surface brightness counterparts (red triangles). This trend follows directly from our redshift-

dependent mapping between  $L$  and halo mass – at fixed stellar mass, the required halo mass increases with redshift (Figure 3) and, as discussed above, more massive halos tend to host more concentrated stellar distributions for a given  $\sigma_*$  and  $L$ . We also see that there is a slight tendency for early-accreted galaxies to be closer to the Sun than more recently-accreted galaxies (middle panel).

The dotted line in the right panel of Figure 4 shows the predicted luminosity function of satellites that are observable for an SDSS-like survey covering the full sky according to the luminosity-distance completeness limits of Walsh et al. (2009). This should be compared to the data points, which reflect the current MW satellite population corrected for sky-coverage as in Tollerud et al. (2008). The uncertainty in the in the sky-coverage correction (associated with the possibility of an anisotropic satellite distribution on the sky) is similar to the size of the points (Tollerud et al. 2008). We see that the predicted and observed populations are roughly consistent. The solid line shows the predicted luminosity function for all satellites within 400 kpc, without any allowance for observational incompleteness. The dashed line, on the other hand, shows the subset of those galaxies that have peak stellar surface densities that are bright enough to be discovered with standard techniques. We see that roughly half of the systems that are in principle luminous enough to be detected with deep surveys like LSST (with  $L \lesssim 1000 L_\odot$ ) have peak surface densities that are too diffuse to be seen. Specifically, even a survey like LSST, with a very deep limiting magnitude, will have difficulties detecting these systems without new observing strategies.

Figure 5 explores how detection bias affects the Strigari plot. In the upper panel, we show  $M_{300}$  vs.  $L$  for all model satellites within 400 kpc of the Sun (color/type

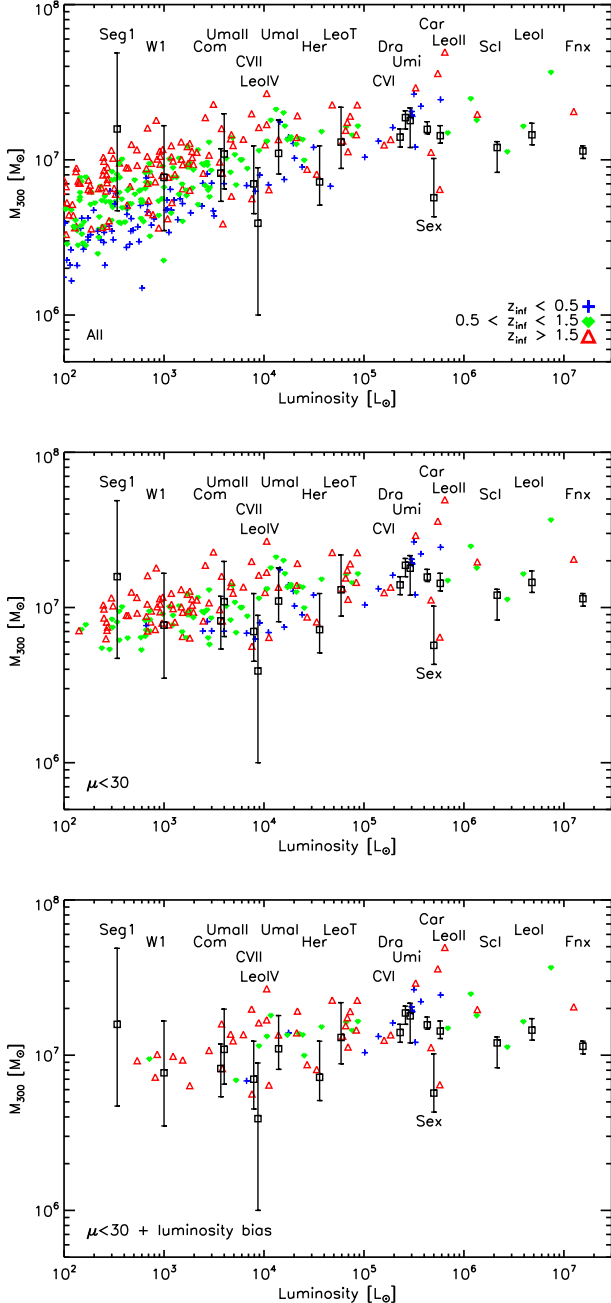


FIG. 5.— Mass within 300 pc as a function of luminosity. Milky Way dSph galaxies are shown as black squares. Fiducial model galaxies are shown as smaller colored points, with the point type and color mapped to the time they fell in to the virial radius of the VL2 main halo. Earlier accretions are red and recent accretions are blue as in Figure 4 and as indicated in the upper panel legend. The *upper panel* presents all predicted satellites and the *middle panel* shows only model satellites that are concentrated enough to be detected with current methods, with  $\mu < 30$  mag arcsec $^{-2}$ . The *bottom panel* includes only the subset of  $\mu < 30$  mag arcsec $^{-2}$  galaxies that are close enough to have been detected by SDSS, according to the 90% completeness limits in Walsh et al. (2009). The  $M_{300}$  masses presented here for MW dSphs are those derived by Strigari et al. (2008). We note that subsequent work has suggested that the velocity dispersion (and hence mass) errors on Hercules (Herc, Adén et al. 2009) and W1 (B. Willman & M. Geha, private communications) are likely underestimated because of membership issues.

scheme is the same as in Figure 4) compared to the MW

dSphs (black squares). We see that unlike the data, there is a significant population of predicted galaxies with low central densities  $M_{300} \lesssim 5 \times 10^6 M_\odot$  for  $L \lesssim 5000 L_\odot$ . Moreover, while the data follow a nearly common-mass relation for  $M_{300}$  vs.  $L$ , the model points prefer a steeper trend:  $M_{300} \propto L^c$  with  $c \simeq 0.15$  (as expected from abundance matching). The model predictions are very similar to those presented in many past CDM-based explorations of satellite  $M_{300}$  values (e.g. Buscha et al. 2009; Muñoz et al. 2009). The similarity between our model results and those of Muñoz et al. (2009), in particular, are encouraging. These authors use the same VL2 catalog that we use, but they explored a more sophisticated model for assigning light to subhalos. Generally, a population of  $L \lesssim 5000 L_\odot$  satellite galaxies with  $M_{300} \lesssim 5 \times 10^6 M_\odot$  seems to be a fairly robust expectation for hierarchical models, especially if  $H_2$  cooling plays a role in the formation stars in surviving galaxy halos at  $z = 0$  (Muñoz et al. 2009).

The middle panel of Figure 5 includes only those model galaxies that have peak surface brightness  $\mu < 30$  mag arcsec $^{-2}$ . We see that this requirement immediately removes the population of  $M_{300} \lesssim 5 \times 10^6 M_\odot$  objects. The lower panel includes only those galaxies that meet both the surface brightness requirement and the luminosity-distance requirement for SDSS discovery. We see that the resultant population of observable model galaxies has  $M_{300}$  values that are very much in line with those of the known MW dSphs. The model we have adopted therefore reproduces both the luminosity function and something close to the mass-luminosity trend seen for Milky Way dwarfs, once all of the relevant selection bias effects are taken into account.

Of course, if the smallest dark matter halos do not contain galaxies at all, then the likelihood for a significant stealth galaxy population is much reduced. We explore this expectation with our Threshold Scenario, which imposes a sharp scale in galaxy formation at  $M_{\text{halo}} = 5 \times 10^8 M_\odot$ . Below this scale dark matter halos are completely devoid of stars (vertical line in Figure 3). The resultant Strigari plot and luminosity functions for this model are shown in Figure 6. Like the Fiducial Scenario, the Threshold Scenario also reproduces the observed satellite luminosity function (right panel). However, unlike in the Fiducial Scenario, we now expect only a handful of stealth galaxies that remain undiscovered (solid vs. dashed lines). The Threshold case also yields a Strigari relation that is in reasonable agreement with the data (left panel), without appealing to any selection bias. Another distinct difference in the Threshold Scenario is that all of the low-luminosity galaxies are expected to be quite old (or at least to have been accreted early  $z_{\text{inf}} > 1.5$ ).

One problem with both of our models is that they produce too many massive dwarf satellites with  $M_{300} \gtrsim 2 \times 10^7 M_\odot$  compared to the data (Figures 5 and 6). This has nothing to do with our method of light assignment. There are simply too many massive subhalos in the VL2 halo when compared to the MW satellite population. The same problem is responsible for the fact that our model galaxies tend to be too small at  $L \gtrsim 10^5 L_\odot$  compared to the data in the left panel of Figure 4. These model galaxies reside in subhalos that are more massive than the subhalos that host the brightest galaxies in the

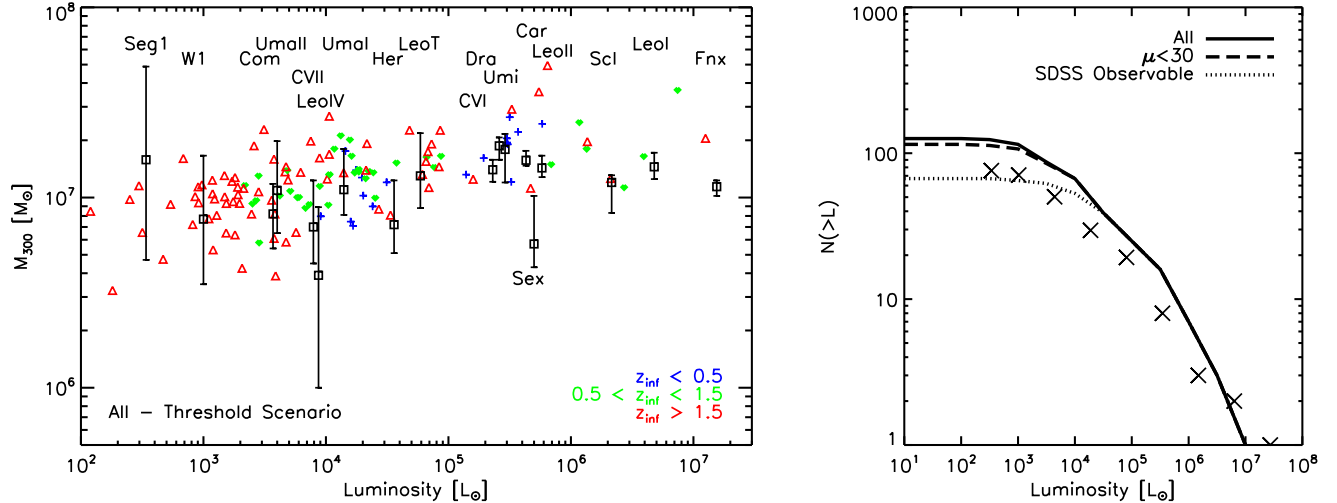


FIG. 6.— Threshold Scenario predictions for the Strigari plot (left) and luminosity function (right). The symbols and line types are identical to those in Figure 5 and the right panel of Figure 4, respectively. This model imposes a sharp truncation in galaxy formation efficiency at  $M_{\text{halo}} = 5 \times 10^8 M_\odot$ , which drastically reduces the expected number of stealth galaxies.

Milky Way, and this confines their stars to a characteristically smaller radius. It is possible that this difference can be attributed to the fact that VL2 represents a slightly more massive halo than the Milky Way’s dark matter halo. It is also possible that it can be explained by cosmic variance in the subhalo populations from galaxy to galaxy.

It is important to mention that the  $M_{300}$  masses in Figures 2, 5 and 6 are taken directly from the spherical Jeans modeling of Strigari et al. (2008). A more recent analysis of membership in the Hercules dwarf (labeled Her in Figures 5 and 6) by Adén et al. (2009) suggests that the actual  $M_{300}$  mass for this system is about a factor of  $\sim 2$  lower than the value we have used. Though this result does not change the fact that there is no strong observed trend between  $M_{300}$  and  $L$  in the data, it does make the mass of Hercules more difficult to explain in our model (and in almost all CDM-based models to date). In the right panel of Figure 2, the Adén et al. (2009) velocity dispersion for Hercules  $\sigma_* \simeq 3.7 \text{ km s}^{-1}$  would shift the point at  $L \simeq 3 \times 10^4 L_\odot$  down to the edge of its error-bar – clearly low enough that this system would not be expected to be stealth according to our definition. The fact that the velocity dispersion shifts this much by removing or adding a few stars suggests that there is a large membership-related systematic error that needs to be taken into account in the mass modeling.<sup>5</sup> More work on the issue of membership and mass modeling in this interesting object is certainly warranted.

## 5. CONCLUSIONS AND DISCUSSION

We have argued that there is likely a population of low-luminosity satellite galaxies orbiting within the halo of the Milky Way that are too diffuse to have been detected with current star-count surveys, despite the fact that they have luminosities similar to those of known ultrafaint MW dSphs. These stealth galax-

ies should preferentially inhabit the smallest dark matter subhalos that host stars ( $V_{\text{max}} \lesssim 15 \text{ km s}^{-1}$ ). One implication is that selection bias (Figures 2 and 5) may play a role explaining the apparent common mass scale for MW dSph galaxies (Strigari et al. 2008; Peñarrubia et al. 2008; Walker et al. 2009; Wolf et al. 2009).

We developed a plausible estimate for the number and character of MW stealth satellites using the subhalo catalogs of the VL2 simulation (Diemand et al. 2008). We assigned light to subhalos by extrapolating the dark matter mass-light relationship required to reproduce bright galaxy number counts (Moster et al. 2009) and we assigned stellar velocity dispersions to each system by adopting the empirical relationship between  $\sigma_*$  and  $L$  for known Milky Way dwarfs. Finally, galaxy sizes were computed using the dynamical relationship between  $R_e$  and  $\sigma_*$  for the measured dark matter halo densities in each subhalo (Equation 3). The resultant model galaxy population includes a substantial fraction of ultrafaint galaxies that are stealth, with peak surface brightness  $\mu > 30 \text{ mag arcsec}^{-2}$ . According to our fiducial estimate, about half of the several hundred satellite galaxies that should be potentially observable by surveys like LSST fall into this category (Figure 4).

We also explored the possibility that there is a sharp threshold in galaxy formation at a halo mass of  $M_{\text{halo}} = 5 \times 10^8 M_\odot$ . This idea follows from the common mass conjecture in Strigari et al. (2008) and remains viable since it reproduces the observed Milky Way satellite luminosity function as well as a fairly weak  $M_{300}$  vs.  $L$  trend without appealing to selection bias (Figure 6). In this scenario, all satellite galaxies are born within halos that are quite dense, and therefore the number of predicted stealth galaxies (which preferentially inhabit the smallest dark matter halos) is significantly reduced (Figure 6). Moreover, we expect that all of the low-luminosity satellites will have been accreted since  $z \simeq 1.5$  (Figure 6) and that they will all host old stellar populations. This is not necessarily the case in our Fiducial Scenario, where the most distant and low-mass subhalos may host ultrafaint

<sup>5</sup> This is not the only systematic uncertainty. As the most elongated of the dSphs known, Hercules is not particularly well suited for spherical Jeans modeling in the first place.



galaxies that contain intermediate-age stars.

It is well known that galaxy formation has a primary mass scale – the scale that gives rise to the  $L_*$  cutoff in galaxy counts at the bright end of the luminosity function. We do not know if there is a second mass scale that operates at the low-luminosity end. One implication of our findings is that a complete search for very low surface brightness satellite galaxies of the Milky Way can help determine whether or not there is a second scale in galaxy formation. If very few stealth galaxies are discovered, this will be an indication that there are no very low mass halos that host stars. A similar effect would be seen if there were simply a truncation in the power spectrum, as might be expected in  $\sim 1$  KeV WDM models (Strigari et al. 2008; Maccio' & Fontanot 2009). In this sense, the discovery of many stealth galaxies in the halo would provide a means to constrain dark matter particle properties in addition to galaxy formation physics.

Kollmeier et al. (2009) have performed kinematic follow-up observations of the Pices Overdensity (also called Structure J) at a distance of  $\sim 85$  kpc and have argued that it may be a very low surface brightness dwarf galaxy. If this is true then it represents the first detection of a stealth dwarf galaxy in the halo of the Milky Way. Unlike the well-known ultrafaint dSphs of the Milky Way, which were discovered as overdensities in RGB or MS turnoff stars, this system was discovered as an excess in RR Lyrae variables in the multi-epoch SDSS Stripe-82 (Watkins et al. 2009; Sesar et al. 2007).

Repeated sky surveys like Pan-STARRS and LSST may provide the best hope for discoveries of this kind in the future. We caution that one potential problem with the stealth-galaxy interpretation of the Pices Overdensity comes from Sharma et al. (in preparation), who have used 2MASS data to show that this structure is consistent with being part of a larger overdensity of stars, in which case it is unlikely to be a bound dwarf. Deeper, wide-field imaging and spectroscopic follow-up will be required to determine the nature of this interesting structure.

It is reassuring to note that upcoming deep, time-resolved sky surveys and associated follow-up campaigns with 30m-class telescopes offer significant hope for the discovery of hundreds of new dwarf galaxy companions of the Milky Way (Tollerud et al. 2008). Confident searches within these data offer a means to constrain the overall count of stealth galaxies that lurk at very low surface brightness and to provide unparalleled constraints on the efficiency of galaxy formation in the smallest dark matter halos.

We thank B. Barton, C. Rockosi, M. Geha, G. Gilmore, J. Simon, L. Strigari, B. Willman, and Joe Wolf for enlightening discussions. M. Geha, J. Simon and L. Strigari provided valuable advice on the manuscript. This work was supported by the Center for Cosmology at the University of California, Irvine.

## REFERENCES

- Adén, D., Wilkinson, M. I., Read, J. I., Feltzing, S., Koch, A., Gilmore, G. F., Grebel, E. K., & Lundström, I. 2009, *ApJL*, Accepted, arXiv:0910.1348
- Belokurov, V., et al. 2007, *ApJ*, 654, 897
- . 2009, *MNRAS*, 397, 1748
- Berrier, J. C., Bullock, J. S., Barton, E. J., Guenther, H. D., Zentner, A. R., & Wechsler, R. H. 2006, *ApJ*, 652, 56
- Bullock, J. S., Kolatt, T. S., Sigad, Y., Somerville, R. S., Kravtsov, A. V., Klypin, A. A., Primack, J. R., & Dekel, A. 2001, *MNRAS*, 321, 559
- Bullock, J. S., Kravtsov, A. V., & Weinberg, D. H. 2000, *ApJ*, 539, 517
- Busha, M. T., Alvarez, M. A., Wechsler, R. H., Abel, T., & Strigari, L. E. 2009, *ApJ*, Submitted, arXiv:0901.3553
- Conroy, C., & Wechsler, R. H. 2009, *ApJ*, 696, 620
- Conroy, C., Wechsler, R. H., & Kravtsov, A. V. 2006, *ApJ*, 647, 201
- Courteau, S., Dutton, A. A., van den Bosch, F. C., MacArthur, L. A., Dekel, A., McIntosh, D. H., & Dale, D. A. 2007, *ApJ*, 671, 203
- Diemand, J., Kuhlen, M., Madau, P., Zemp, M., Moore, B., Potter, D., & Stadel, J. 2008, *Nature*, 454, 735
- Geha, M., Willman, B., Simon, J. D., Strigari, L. E., Kirby, E. N., Law, D. R., & Strader, J. 2009, *ApJ*, 692, 1464
- Grillmair, C. J. 2006, *ApJ*, 645, L37
- . 2009, *ApJ*, 693, 1118
- Ivezic, Z., et al. 2008, arXiv:0805.2366
- Kazantzidis, S., Mayer, L., Mastrogiuseppe, C., Diemand, J., Stadel, J., & Moore, B. 2004, *ApJ*, 608, 663
- Kirby, E. N., Simon, J. D., Geha, M., Guhathakurta, P., & Frebel, A. 2008, *ApJ*, 685, L43
- Klypin, A., Kravtsov, A. V., Valenzuela, O., & Prada, F. 1999, *ApJ*, 522, 82
- Kollmeier, J. A., et al. 2009, *ApJ*, 705, L158
- Koposov, S., et al. 2008, *ApJ*, 686, 279
- Kravtsov, A. V. 2009, arXiv:0906.3295
- Kravtsov, A. V., Berlind, A. A., Wechsler, R. H., Klypin, A. A., Gottlöber, S., Allgood, B., & Primack, J. R. 2004, *ApJ*, 609, 35
- Li, Y., Helmi, A., De Lucia, G., & Stoehr, F. 2009, *MNRAS*, 397, L87
- Maccio', A. V., & Fontanot, F. 2009, arXiv:0910.2460
- Macciò, A. V., Kang, X., & Moore, B. 2009, *ApJ*, 692, L109
- Majewski, S. R., et al. 2007, *ApJ*, 670, L9
- Marín, F. A., Wechsler, R. H., Frieman, J. A., & Nichol, R. C. 2008, *ApJ*, 672, 849
- Martin, N. F., de Jong, J. T. A., & Rix, H.-W. 2008, *ApJ*, 684, 1075
- Martin, N. F., Ibata, R. A., Chapman, S. C., Irwin, M., & Lewis, G. F. 2007, *MNRAS*, 380, 281
- Martin, N. F., et al. 2009, *ApJ*, 705, 758
- Moore, B., Ghigna, S., Governato, F., Lake, G., Quinn, T., Stadel, J., & Tozzi, P. 1999, *ApJ*, 524, L19
- Moster, B. P., Somerville, R. S., Maubetsch, C., van den Bosch, F. C., Maccio', A. V., Naab, T., & Oser, L. 2009, *ApJ*, Submitted, arXiv:0903.4682
- Muñoz, J. A., Madau, P., Loeb, A., & Diemand, J. 2009, *MNRAS*, Accepted, arXiv:0905.4744
- Navarro, J. F., Frenk, C. S., & White, S. D. M. 1997, *ApJ*, 490, 493
- Okamoto, T., & Frenk, C. S. 2009, *MNRAS*, L315+
- Peñarrubia, J., McConnachie, A. W., & Navarro, J. F. 2008, *ApJ*, 672, 904
- Pryor, C., & Meylan, G. 1993, in *Astronomical Society of the Pacific Conference Series*, Vol. 50, *Structure and Dynamics of Globular Clusters*, ed. S. G. Djorgovski & G. Meylan, 357–+
- Purcell, C. W., Bullock, J. S., & Zentner, A. R. 2007, *ApJ*, 666, 20
- Sesar, B., et al. 2007, *AJ*, 134, 2236
- Simon, J. D., & Geha, M. 2007, *ApJ*, 670, 313
- Spergel, D. N., et al. 2007, *ApJS*, 170, 377
- Springel, V., et al. 2008, *MNRAS*, 391, 1685
- Stark, D. V., McGaugh, S. S., & Swaters, R. A. 2009, *AJ*, 138, 392
- Stewart, K. R., Bullock, J. S., Barton, E. J., & Wechsler, R. H. 2009, *ApJ*, 702, 1005
- Stewart, K. R., Bullock, J. S., Wechsler, R. H., Maller, A. H., & Zentner, A. R. 2008, *ApJ*, 683, 597
- Stoehr, F., White, S. D. M., Tormen, G., & Springel, V. 2002, *MNRAS*, 335, L84

- Strigari, L. E., Bullock, J. S., Kaplinghat, M., Diemand, J., Kuhlen, M., & Madau, P. 2007, *ApJ*, 669, 676
- Strigari, L. E., Bullock, J. S., Kaplinghat, M., Simon, J. D., Geha, M., Willman, B., & Walker, M. G. 2008, *Nature*, 454, 1096
- Stringer, M., Cole, S., & Frenk, C. 2009, *ArXiv e-prints*
- Tasitsiomi, A., Kravtsov, A. V., Wechsler, R. H., & Primack, J. R. 2004, *ApJ*, 614, 533
- Tollerud, E. J., Bullock, J. S., Strigari, L. E., & Willman, B. 2008, *ApJ*, 688, 277
- Vale, A., & Ostriker, J. P. 2004, *MNRAS*, 353, 189
- Walker, M. G., Mateo, M., Olszewski, E. W., Peñarrubia, J., Wyn Evans, N., & Gilmore, G. 2009, *ApJ*, 704, 1274
- Walsh, S. M., Willman, B., & Jerjen, H. 2009, *AJ*, 137, 450
- Watkins, L. L., et al. 2009, *MNRAS*, 398, 1757
- Willman, B., et al. 2005, *ApJ*, 626, L85
- Wolf, J., Martinez, G. D., Bullock, J. S., Kaplinghat, M., Geha, M., Munoz, R. R., Simon, J. D., & Avedo, F. F. 2009, *MNRAS*, submitted, arXiv:0908.2995
- Zentner, A. R., & Bullock, J. S. 2003, *ApJ*, 598, 49
- Zucker, D. B., et al. 2006, *ApJ*, 643, L103